New Miniaturized Dual-Band Rat-Race Coupler With Microwave *C*-Sections

Yi-Chyun Chiou, Jen-Tsai Kuo, and Chi-Hung Chan

Department of Communication Engineering, National Chiao Tung University, Hsinchu 300 TAIWAN

***Abstract*—Based on microwave *C*-sections, rat-race coupler is designed to have a dual-band characteristic and a miniaturized area. The *C*-section together with two transmission line sections attached to both of its ends is synthesized to realize a phase change of 90° at the first frequency, and 270° at the second passband. The equivalence is established by the transmission line theory, and transcendental equations are derived to determine its structure parameters. Two circuits are realized in this presentation; one is designed at 2.45/5.2 GHz and the other at 2.45/5.8 GHz. The latter circuit occupies only 31% of the area of a conventional hybrid ring at the first band. It is believed that this circuit has the best size reduction for microstrip dual-band rat-race couplers in open literature. The measured results show good agreement with simulation responses.**

***Index Terms*—Microwave *C*-section, dual-band, microstrip line, miniaturization, rat-race coupler.**

I. INTRODUCTION

In the RF frond-end of a modern communication system, hybrid couplers are one of the most important devices [1]. They are widely used in several microwave and millimeter wave sub-systems such as balanced amplifiers and mixers. In the past few decades, a series of innovative synthesis and design have been proposed for these couplers [2]-[5]. In [2], simple formulation is devised to design the ring coupler. In [3], a rigorous synthesis procedure is demonstrated for branch-line couplers with equal power division. In [4], a rat-race coupler consisting of cascade structure of alternative high- and low-impedance transmission lines is presented to achieve a large power split ratio over a wide bandwidth. On the basis of design equations in [4], a miniaturized periodic stepped-impedance rat-race coupler with arbitrary power division ratio can be realized [5]. Note that all couplers in [2]-[5] are designed for operation at a single band.

Recent rapid progress in wireless communications has created a need of dual-band operation for RF devices, such as the global systems for mobile communication systems (GSM) at 0.9/1.8 GHz and wireless local area network (WLAN) at 2.4/5.2 GHz. Recently, numerous research papers on dual-band hybrid couplers have been published [6]-[13]. In [6], a planar dual-band branch-line coupler with a compact circuit area is proposed. Each quarter wavelength (λ/4) section is replaced by a short transmission line section with a pair of shunt short-circuited or open stubs attached to its ends. Based on a similar circuit structure, a rat-race coupler with two arbitrary operation frequencies is presented in [7]. An alternative branch-line coupler for dual-band operation is introduced in [8]. The circuit consists of cross branches that offer extra degrees of freedom to achieve the design. In [9], a tapped open stub is used to contrive a dual-band branch-line coupler. The two bands can be arbitrarily designated by adequately tuning the length and characteristic impedance of the stub. In [10], a stepped-impedance line section with two open stubs is proposed to establish a dual-band rat-race coupler. In [11], four identical open stubs are devised for design of a novel dual-band rectangular patch hybrid coupler.

The metamaterial approach [12]-[13] can also be used to implement couplers with the dual-band operation. In [12], arbitrary dual-band components such as branch-line and rat-race couplers are realized by composite right- and left-handed transmission line (CRLH TL) sections. Dual-band devices are also carried out on the basis of the simplified CRLH TL [13]. So far, however, it is still a challenge to design a miniaturized dual-band rat-race coupler. In [14], dual-band couplers with arbitrary power division ratios are presented. Each transmission line section consists of a stepped-impedance line section with open stubs tapped with its both ends. Rigorous design procedure is described and several circuits operating at 2.45/5.2 GHz are realized. To the best of our knowledge, it is the first miniaturized dual-band coupler with arbitrary power divisions at two designated bands in open literature.

In this paper, a miniaturized dual-band rat-race coupler is implemented with the microwave *C*-sections. Each λ/4 section of a conventional rat-race coupler is replaced by the proposed elementary two-port which consists of two line sections with a *C*-section in between. Design equations are formulated by establishing the equivalence between the two-port and the λ/4 section at two frequencies. To facilitate the circuit design, some design graphs are provided.

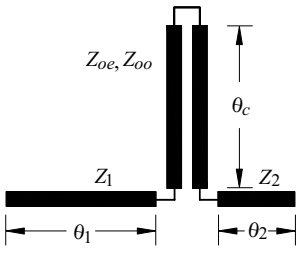

Fig. 1. The proposed elementary two-port with a *C*-section.

II. Elementary Two-Port for Dual-Band Operation

Figure 1 shows the proposed elementary two-port network for the dual-band operation. The two-port is built with two transmission line segments of lengths θ_1 and θ_2 and characteristic impedances Z_1 and Z_2 with a microwave *C*-section of length θ_c in the middle. Since the phase-shift of the *C*-section is nonlinear with respect to frequency [15], it is suitable for realizing the dual-band function.

Let the two designated operation frequencies be f_1 and $f_2 = nf_1$. In our approach, the six λ/4 sections of the traditional coupler are replaced by the proposed two-port. For simplicity, let $Z_1 = Z_2 = \sqrt{Z_{oe}Z_{oo}}$, where Z_{oe} and Z_{oo} are the even- and odd-mode characteristic impedances of the coupled-line, respectively. By enforcing the *ABCD* matrix of the two-port to be equal to those of a uniform transmission line section of 90° and 270° at f_1 and f_2, respectively, the following four equations can be readily obtained:

$$P(\theta_c)\cos\theta + 2Z_1\sin\theta = 0 \tag{1a}$$

$$P(\theta_c)\sin\theta - 2Z_1\cos\theta = Q(\theta_c)\times Z_T/Z_1 \tag{1b}$$

$$P(n\theta_c)\cos n\theta + 2Z_1\sin n\theta = 0 \tag{1c}$$

$$P(n\theta_c)\sin n\theta - 2Z_1\cos n\theta = -Q(n\theta_c)\times Z_T/Z_1 \tag{1d}$$

where

$$P(\theta_c) = Z_{oo}\tan\theta_c - Z_{oe}\cot\theta_c \tag{2a}$$

$$Q(\theta_c) = -(Z_{oo}\tan\theta_c + Z_{oe}\cot\theta_c) \tag{2b}$$

In (1) and (2), $\theta = \theta_1 + \theta_2$, Z_o is the reference impedance, and $Z_T = \sqrt{2}Z_o$ is the characteristic impedance of the six λ/4 sections of a conventional hybrid ring. After some algebraic manipulations, the following equations can be obtained for determination of Z_{oe} and Z_{oo}:

$$Z_T \times Z_{oe}(f_1) = Z_1^2\sec\theta\tan\theta_c + Z_1\tan\theta\tan\theta_c \tag{3a}$$

$$Z_T \times Z_{oo}(f_1) = Z_1^2\sec\theta\cot\theta_c - Z_1\tan\theta\cot\theta_c \tag{3b}$$

$$Z_T \times Z_{oe}(f_2) = Z_T Z_1\tan n\theta\tan n\theta_c - Z_1^2\sec n\theta\tan n\theta_c \tag{3c}$$

$$Z_T \times Z_{oo}(f_2) = -Z_T Z_1\tan n\theta\cot n\theta_c - Z_1^2\sec n\theta\cot n\theta_c \tag{3d}$$

One can validate that $Z_{oe}(f_1)Z_{oo}(f_1) = Z_{oe}(f_2)Z_{oo}(f_2) = Z_1^2$ when $Z_1 = Z_T$. Here, the dispersion of microstrip characteristic impedance is neglected. Once n, θ_c and θ are given, by enforcing $Z_{oe}(f_1) = Z_{oe}(f_2)$ or $Z_{oo}(f_1) = Z_{oo}(f_2)$, the structure parameters of the dual-band element can be solved as follows. Figure 2(a) plots the changes of $Z_{oe}(f_1)$ and $Z_{oe}(f_2)$ with respect to the variation of θ for $\theta_c = 50^o$, 47.5^o and 45^o for $n = 2.12$. This specific n value is used when $f_1 = 2.45$ GHz and $f_2 = 5.2$ GHz. As shown in Fig. 2(a), when θ_c is decreased from 50^o to 45^o, the Z_{oe} solution, i.e. the intersected points, is increased. When $\theta_c = 45°$, the solution reads $Z_{oe} = 130\ \Omega$ and $Z_{oo} = 2Z_o^2/Z_{oe} = 38.45\ \Omega$. Implemented by coupled microstrips, the gap size over substrate thickness ratio S/h will be 0.08 for a substrate with $\varepsilon_r = 10.2$. When the substrate thickness $h = 1$ mm, such gap sizes will be critical for microstrip realization by the standard fabrication process since it is close to being beyond the resolution limit. One may increase θ_c to release the tight gap size as indicated in Fig. 2(a). Figure 2(b) draws the $Z_{oe}(f_1)$ and $Z_{oe}(f_2)$ solutions against the variation of θ for $n = 2.1, 2.2, \ldots, 3$ for $\theta_c = 45°$. When n is increased, the Z_{oe} solution decreases. Note that when $\theta = 0$ and $n = 3$, the solution $Z_{oe} = 70.7\ \Omega$. It validates the fact that when the two-port is used to imitate a λ/4 section at f_1 and 3λ/4 at $f_2 = 3f_1$, the *C*-section becomes a folded section with $Z_{oe} = Z_{oo}$.

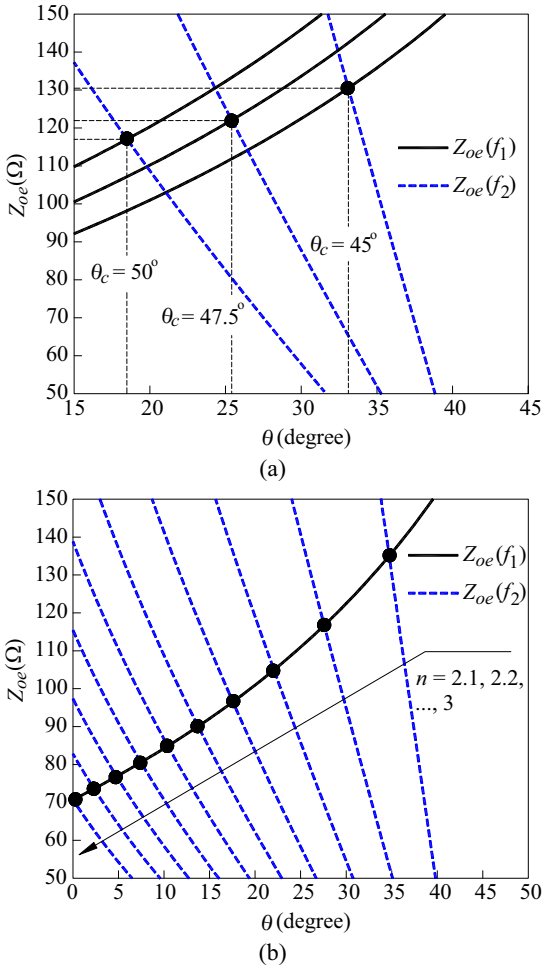

Fig. 2. $Z_{oe}(f_1)$ and $Z_{oe}(f_2)$ against the variation of θ, where $Z_1 = 70.7\ \Omega$. (a) $n = 2.12$. (b) $\theta_c = 45°$.

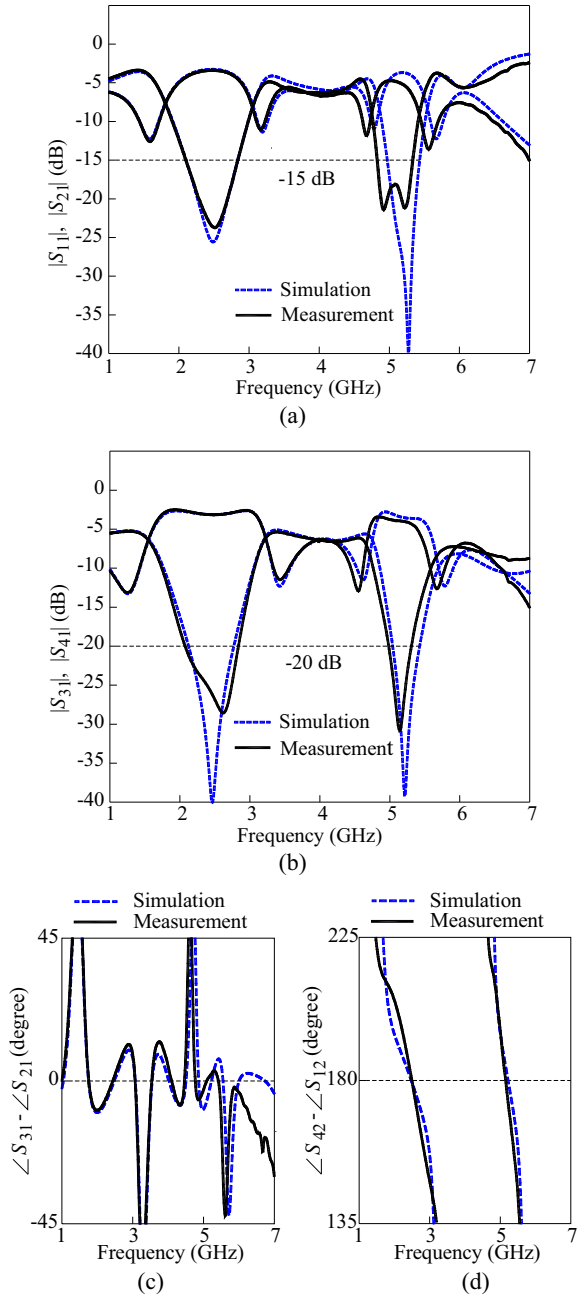

Fig. 3. Simulated and measured responses of the fabricated rat-race coupler at 2.45/5.2 GHz. (a) $|S_{11}|$ and $|S_{21}|$. (b) $|S_{31}|$ and $|S_{41}|$. (c) $\angle S_{31} - \angle S_{21}$. (d) $\angle S_{42} - \angle S_{12}$. $n = 2.12$, $\theta_c = 48°$, $\theta = 23.85°$, $Z_1 = 70.7\ \Omega$, $Z_{oe} = 120.65\ \Omega$ and $Z_{oo} = 41.45\ \Omega$.

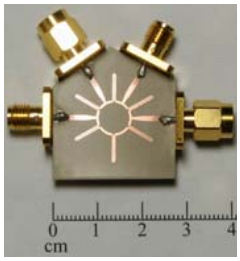

Fig. 4. Photograph of the dual-band rat-race.

III. Simulation and Measurement

Two rat-race couplers designed at 2.45/5.2 GHz and 2.45/5.8 GHz are fabricated and measured for demonstration Figures 3 and 4 show the simulated and measured results. The circuit has a substrate of $\varepsilon_r = 10.2$ and $h = 1.27$ mm. Simulation data are obtained by the electromagnetic software package IE3D [16]. Figure 3(a) plots $|S_{11}|$ and $|S_{21}|$ responses. It can be observed that all measured $|S_{11}|$ at both the designated frequencies are better than 18 dB. If a 15-dB return loss is referred, measured data indicate that the circuit has bandwidths of 30% and 9% at f_1 and f_2, respectively. Figure 3(b) shows the $|S_{31}|$ and $|S_{41}|$ curves. The measured isolations $|S_{41}|$ at f_1 and f_2 are better than 25 dB. For a 20-dB reference, the measured isolations possess bandwidths of 27% and 8% at f_1 and f_2, respectively. Also, detailed data show that the total power loss of the circuit $P_L = 1 - |S_{11}|^2 - |S_{21}|^2 - |S_{31}|^2 - |S_{41}|^2$ at f_1 and f_2 are 4% and 8.2%, respectively.

Figures 3(c) and 3(d) plot the responses of relative phase $\angle S_{31} - \angle S_{21}$ and $\angle S_{42} - \angle S_{12}$, respectively. One can observe that these responses have relatively smooth variations over the first band as compared with those over the second. It reflects the fact that the circuit has a bandwidth at f_1 larger than that at f_2. Good agreement between the simulation and measured responses for the experiment circuits can be observed. Figure 4 shows the photograph of the experimental circuit.

Figures 5(a) and 5(b) plot the magnitude responses of S_{11}, S_{21}, S_{31} and S_{41} of the second experimental dual-band rat-race. At both f_1 and f_2, the measured $|S_{11}|$ results are better than 20 dB. The measurement indicates that the circuit has bandwidths of 37% and 8% at f_1 and f_2, respectively, for a 15-dB return loss. These bandwidths are closely related to the relative phases $\angle S_{31} - \angle S_{21}$ and $\angle S_{42} - \angle S_{12}$ shown in Fig. 5(c) and 5(d), respectively. The experimental $|S_{41}|$ data show that the isolations are better than 35 dB, and the total power losses P_L are 3.2% and 7.3% at f_1 and f_2, respectively.

Figure 6 shows the photograph of the experimental circuit. In this design, all the *C*-sections can be placed inside the ring circumference. This is because this circuit has a larger n value than the previous one so that the θ_c solution shown in Fig. 2 can be shorter. It occupies only 31% of the area of a conventional rat-race coupler. It is believed that this circuit has the best size reduction comparing with the microstrip dual-band rat-race couplers in open literature.

IV. Conclusion

The function of a microwave *C*-section is exploited for dual-band and circuit miniaturization. For design of a dual-band rat-race coupler, the *C*-section together with two short microstrip sections at its ends is used to replace each of the six λ/4 sections of a traditional coupler at the two design frequencies. This approach can save more than 69% of the circuit area. The proposed two-port is viable for development of other dual-band microwave passive devices.

ACKNOWLEDGEMENT

This work was supported in parts by the ATU program of MoE and by the National Science Council, Taiwan, under the Grant NSC 97-2221-E-009-039 and NSC 98-2218-E-009-011.

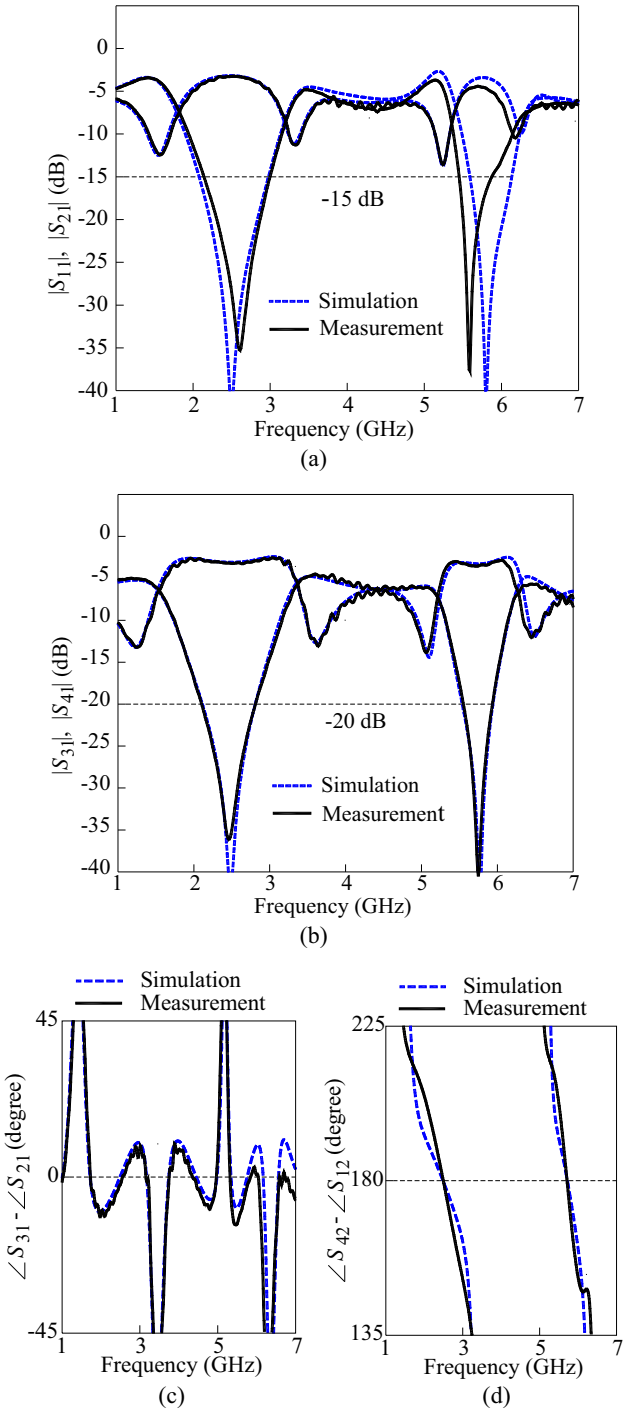

Fig. 5. Simulated and measured responses of the fabricated dual-band rat-race coupler at 2.45/5.8 GHz. (a) $|S_{11}|$ and $|S_{21}|$. (b) $|S_{31}|$ and $|S_{41}|$. (c) $\angle S_{31} - \angle S_{21}$. (d) $\angle S_{42} - \angle S_{12}$. n = 2.37, θ_c = 36.5°, θ = 43.22°, Z_1 = 70.7 Ω, Z_{oe} = 121 Ω and Z_{oo} = 41.33 Ω.

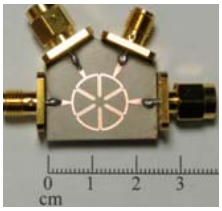

Fig. 6. Photograph of the fabricated 2.45/5.8 GHz rat-race coupler.

REFERENCES

[1] D. M. Pozar, *Microwave Engineering*, 3rd ed. New York: Wiley, 2005.

[2] C. Y. Pon, "Hybrid-ring directional coupler for arbitrary power division," *IEEE Trans. Microw. Theory Tech.*, vol. 19, no. 11, pp. 529-535, Nov. 1961.

[3] R. Levy and L. J. Lind, "Synthesis of symmetric branch line guide directional couplers," *IEEE Trans. Microw. Theory Tech.*, vol. 16, no. 12, pp. 80-89, Dec. 1968.

[4] A. K. Agrawal and G. F. Mikucki, "A printed-circuit hybrid-ring directional coupler for arbitrary power divisions," *IEEE Trans. Microw. Theory Tech.*, vol. 34, no. 12, pp. 1401-1407, Dec. 1986.

[5] Y.-C. Chiou, J.-S. Wu and Jen-Tsai Kuo, "Periodic stepped-impedance rat race coupler with arbitrary power division," *Proc. 2006 Asia-Pacific Microw. Conf.*, pp. 663-666, Dec. 2006.

[6] K.-K. M. Cheng and F.-L. Wong, "A novel approach to the design and implementation of dual-band compact planar 90° branch-line coupler," *IEEE Trans. Microw. Theory Tech.*, vol. 52, no. 11, pp. 2458-2463, Nov. 2004.

[7] K.-K. M. Cheng and F.-L. Wong, "A novel rat race coupler design for dual-band applications," *IEEE Microw. Wireless Compon. Lett.*, vol. 15, no. 8, pp. 521-523, Aug. 2005.

[8] M.-J. Park and B. Lee, "Dual-band cross-coupled branch line coupler," *IEEE Microw. Wireless Compon. Lett.*, vol. 15, no. 10, pp. 655-657, Oct. 2005.

[9] H. Zhang and K. J. Chen, "A stub tapped branch-line coupler for dual-band operations," *IEEE Microw. Wireless Compon. Lett.*, vol. 17, no. 2, pp. 106-108, Feb. 2007.

[10] C.-L. Hsu, C.-W. Chang and J.-T. Kuo, "Design of dual-band microstrip rat race coupler with circuit miniaturization," *IEEE MTT-S Int. Microw. Symp. Dig.*, pp. 177-180, Jun. 2007.

[11] S. Y. Zheng, S. H. Yeung, W. S. Chan, K. F. Man, S. H. Leung and Q. Xue, "Dual-band rectangular patch hybrid coupler," *IEEE Trans. Microw. Theory Tech.*, vol. 56, no. 71, pp. 1721-1728, Jul. 2008.

[12] I.-H. Lin, M. Devincentis, C. Caloz and T. Itoh, "Arbitrary dual-band components using composite right/left-handed transmission lines," *IEEE Trans. Microw. Theory Tech.*, vol. 52, no.4, pp. 1142-1149, Apr. 2004.

[13] X. Q. Lin, R. P. Liu, X. M. Yang, J. X. Chen, X. X. Ying, Q. Cheng and T. J. Cui, "Arbitrary dual-band components using simplified structures of conventional CRLH TLs," *IEEE Trans. Microw. Theory Tech.*, vol. 54, no. 7, pp. 2902-2909, Jul. 2006.

[14] C.-L. Hsu, J.-T. Kuo and C.-W. Chang, "Miniaturized dual-band hybrid couplers with arbitrary power division ratios," *IEEE Trans. Microw. Theory Tech.*, vol. 57, no. 1, pp. 149-156, Jan. 2009.

[15] M. M. Schiffman, "A new class of broad-band microwave 90-degree phase shifter," *IRE Trans. Microw. Theory Tech.*, vol. 6, no. 6, pp. 232-237, Apr. 1958.

[16] *IE3D Simulator*, Zeland Software Inc., Jan. 1997.